Thermally Induced Long-Term Displacement of Thermoactive Piles

Cesar Pasten, A.M.ASCE[1]; and J. Carlos Santamarina, A.M.ASCE[2]

Abstract: The long-term displacement of thermoactive piles subjected to static load and thermal cycles is analyzed using the numerical solution of the one-dimensional load-transfer method modified to account for thermoelastic effects. Numerical results show that thermal cycles cause changes in load transfer and may lead to gradual plastic displacement accumulation due to the mobilization of side shear resistance with the number of thermal cycles. Displacement accumulation depends on the static factor of safety, the amplitude of the thermal cycles, and the ratio between the shaft resistance and the ultimate pile capacity. **DOI: 10.1061/(ASCE)GT.1943-5606.0001092.** © *2014 American Society of Civil Engineers.*

Author keywords: Thermoactive piles; Shakedown; Thermal cycles; Pile-soil interaction.

Introduction

Thermoactive piles can reduce fossil fuel consumption for low-grade energy needs, such as heating and air conditioning in buildings. Thermoactive piles are structural elements equipped with pipe loops connected to a heat pump to exchange heat between a building and the soil mass surrounding the foundation. The thermal inertia of the soil mass absorbs excess heat released from the building during the summer and returns heat to the building during the winter (Brandl 2006).

Pile heating or cooling alters the pile-soil interaction (Amatya et al. 2012; Bourne-Webb et al. 2012; Knellwolf et al. 2011; Laloui et al. 2006; McCartney 2011). Effects may include thermally driven soil consolidation and creep, changes in effective stress, altered pile group response, and differential pile-soil settlement.

In this study, the long-term response of a single pile subjected to thermal cycles relative to the surrounding soil mass is explored. The analysis is based on a one-dimensional load-transfer formulation modified to consider thermoplastic effects. The influence of material parameters, pile type, building static load, and factor of safety as well as the number of thermal cycles are examined for various temperature change amplitudes.

Numerical Algorithm for Cyclic Thermal Loading

The one-dimensional pile-soil load-transfer method (Coyle and Reese 1966; Poulos and Davis 1980) is modified to account for temperature changes.

Element-Level Equilibrium and Compatibility

Consider a pile length L (m) and diameter D (m) discretized into N elements of length $L_0 = L/N$ (m) so that there are $(N + 1)$ interfaces. The static axial force applied on the pile head is $Q_1 = Q^{\text{head}}$ (N) [Fig. 1(a)]. Force equilibrium requires that the axial force on the ith-element upper interface Q_i (N) equals the sum of the axial force on its lower interface Q_{i+1} (N) and the mobilized shaft resistance S_i (N)

$$Q_i = Q_{i+1} + S_i \tag{1}$$

where the shaft resistance S_i = mobilized side friction acting on the ith-element s_i (Pa) times the element contact area

$$S_i = s_i \cdot \pi \cdot D \cdot L_0 \tag{2}$$

The side friction s_i (Pa) is assumed to have a linear elastic-perfectly plastic displacement response

$$s_i = s_i(\delta_i, \delta_{i+1}) = \begin{cases} -s_i^{\text{ult}} & \text{if } \left(\frac{\delta_i + \delta_{i+1}}{2}\right) \le -\delta_s^* \\ k_i \cdot \left(\frac{\delta_i + \delta_{i+1}}{2}\right) & \text{if } -\delta^* < \left(\frac{\delta_i + \delta_{i+1}}{2}\right) < \delta_s^* \\ s_i^{\text{ult}} & \text{if } \delta_s^* \le \left(\frac{\delta_i + \delta_{i+1}}{2}\right) \end{cases} \tag{3}$$

where δ_i (m) and δ_{i+1} (m) = relative pile-soil displacements at the element upper and lower interfaces; $k_i = s_i^{\text{ult}}/\delta_s^*$ (Pa/m) is the shaft stiffness; and δ_s^* (m) = critical relative displacement to mobilize the pile-soil shear strength s_i^{ult} (Pa). The pile-soil shear strength at the ith-element $s_i^{\text{ult}} = \sigma'_{vi} \cdot K_0 \cdot \mu$ combines the vertical effective stress σ'_{vi} (Pa), the coefficient of horizontal stress K_0 [-], and the pile-soil interface friction coefficient μ [-].

Consider a uniform pile temperature increase. Thermal expansion of the ith element is constrained by the change in axial forces acting on the element. Displacement compatibility requires that the change in the element length $\Delta_i = \delta_{i+1} - \delta_i$ (m) equals the free

[1]Assistant Professor, Dept. of Civil Engineering, Univ. of Chile, Av. Blanco Encalada 2002, Santiago 8370449, Chile (corresponding author). E-mail: cpasten@ing.uchile.cl

[2]Professor, School of Civil and Environmental Engineering, Georgia Institute of Technology, 790 Atlantic Dr. NW, Atlanta, GA 30332-0355. E-mail: jcs@gatech.edu

Note. This manuscript was submitted on December 22, 2012; approved on December 30, 2013; published online on January 27, 2014. Discussion period open until June 27, 2014; separate discussions must be submitted for individual papers. This technical note is part of the ***Journal of Geotechnical and Geoenvironmental Engineering***, © ASCE, ISSN 1090-0241/06014003(5)/$25.00.

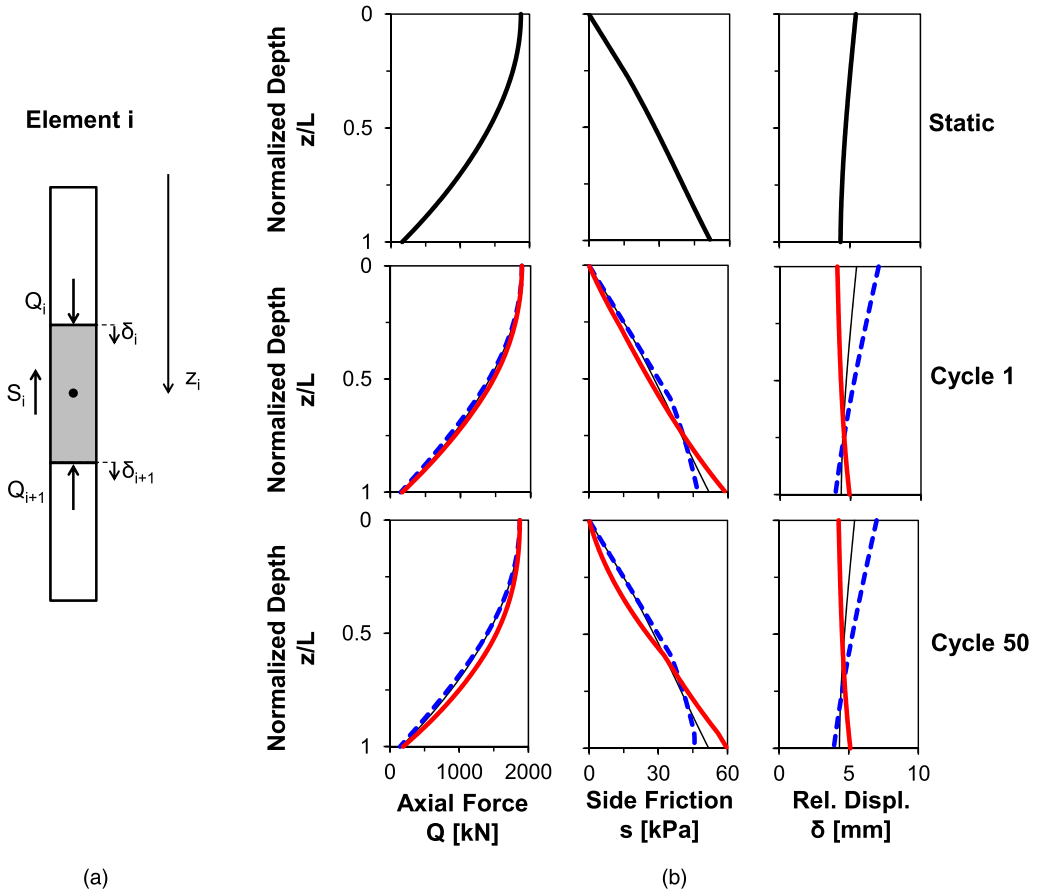

Fig. 1. Load-transfer curves after static loading and thermal cycling: (a) axial forces Q and shaft resistance S acting on the ith element cause interface relative displacements δ; ith element middle point is at depth z_i; (b) axial force Q, side friction s, and relative displacement δ are calculated as a function of the normalized depth z/L for $\Delta T = 20°C$, $Q^{ult} = 3{,}750$ kN, $S^{ult}/Q^{ult} = 0.5$, and $Q^{head}/Q^{ult} = 0.5$, i.e., FS = 2.0; continuous curves correspond to the heating phase and dotted lines to the cooling phase; note that pile parameters are found in Table 2; pile segments $N = 100$

thermal elongation Δ_i^T (m) minus the elastic mechanical contraction Δ_i^σ (m) from the initial unloaded condition

$$\Delta_i = \delta_{i+1} - \delta_i = \Delta_i^T - \Delta_i^\sigma \tag{4}$$

The free thermal elongation $\Delta_i^T = \alpha \cdot \Delta T \cdot L_0$ is computed with the thermal expansion coefficient $\alpha(°C^{-1})$, the temperature change amplitude ΔT (°C), and the element length L_0 (m). The elastic mechanical contraction is

$$\Delta_i^\sigma = \frac{Q_i + Q_{i+1}}{2}\frac{L_0}{A \cdot E} \tag{5}$$

where $A = \pi \cdot D^2/4\,(m^2)$ is the pile's transverse area; and E (Pa) = pile's Young's modulus.

Combining equilibrium and compatibility conditions [Eqs. (1) and (4)], the displacement of the ith-element upper interface δ_i is obtained as a function of the ith-element lower interface displacement δ_{i+1} and axial force Q_{i+1}

$$\delta_i(\delta_{i+1}, Q_{i+1}) = \begin{cases} \delta_{i+1} + \dfrac{L_0}{2AE}\left(2Q_{i+1} - \pi D L_0 s_i^{ult}\right) - \Delta_i^T & \text{if } \left(\dfrac{\delta_i + \delta_{i+1}}{2}\right) \le -\delta_s^* \\ \dfrac{\delta_{i+1}\left(1 + \dfrac{L_0^2 \pi D k_i}{4AE}\right) + \dfrac{L_0}{AE}Q_{i+1} - \Delta_i^T}{1 - \dfrac{L_0^2 \pi D k_i}{4AE}} & \text{if } -\delta_s^* < \left(\dfrac{\delta_i + \delta_{i+1}}{2}\right) < \delta_s^* \\ \delta_{i+1} + \dfrac{L_0}{2AE}\left(2Q_{i+1} + \pi D L_0 s_i^{ult}\right) - \Delta_i^T & \text{if } \delta_s^* \le \left(\dfrac{\delta_i + \delta_{i+1}}{2}\right) \end{cases} \tag{6}$$

The pile tip resistance Q_{N+1} (N) is assumed to be linear elastic–perfectly plastic with a constant critical relative displacement δ_t^* (m) required to mobilize the ultimate tip resistance Q_t^{ult} (N)

$$Q_{N+1} = Q_{N+1}(\delta_{N+1}) = \begin{cases} \left(\frac{Q_t^{\text{ult}}}{\delta_t^*}\right)\delta_{N+1} & \text{if } 0 < \delta_{N+1} < \delta_t^* \\ Q_t^{\text{ult}} & \text{if } \delta_t^* < \delta_{N+1} \end{cases} \quad (7)$$

Finally, the ultimate pile capacity Q^{ult} (N) is the sum of the shaft and the tip resistances

$$Q^{\text{ult}} = S^{\text{ult}} + Q_t^{\text{ult}} \quad (8)$$

and the static factor of safety (FS) for the pile is $Q^{\text{ult}}/Q^{\text{head}}$.

Numerical Algorithm

Eqs. (1)–(7) allow tracking of the evolution of the pile axial force and displacement during thermal cycles. The equilibrium condition for the pile when subjected to a constant temperature change, ΔT, is calculated from the lowest interface at the pile tip $i = (N + 1)$ to the first interface at the pile head $i = 1$. The iterative algorithm follows:

1. Impose a relative displacement at the Nth-element lower interface δ_{N+1} and compute the corresponding tip resistance Q_{N+1} [Eq. (7)].
2. Compute the relative displacement at the Nth-element upper interface δ_N [Eq. (6)].
3. Calculate the Nth-element shaft resistance S_N [Eqs. (2) and (3)] and axial force on its upper interface Q_N [Eq. (1)].
4. Continue element by element to reach the first interface $i = 1$.
5. Compare the computed value of the longitudinal force on the first interface Q_1 with the applied static force Q^{head}. If $|Q_1 - Q^{\text{head}}| > \varepsilon$, where ε (N) is a preselected tolerance value, the iterative procedure is repeated for a different relative displacement δ_{N+1} in Step 1. If $|Q_1 - Q^{\text{head}}| \leq \varepsilon$, the solution has converged.

The load-transfer curves for the static load without heating are obtained using $\Delta_i^T = 0$ in Eq. (4). The application of thermal cycles is imposed once the static load at the pile head is equilibrated. Thermal cycles consist of a sequence of positive or negative temperature changes using the algorithm described previously. Table 1 identifies the governing dimensionless ratios.

Observations

As implemented, the algorithm does not reflect radial strains (mechanical or thermal) or thermomechanical effects in the surrounding soil. The formulation resembles the approach by Knellwolf et al. (2011); however, their algorithm invokes a constant interfacial stiffness (a constant critical interface displacement was imposed in this study; hence, stiffness increases with depth), uses a bilinear interfacial model that allows for plastic displacement in the second linear branch (the formulation in this study involves a simpler linear elastic–perfectly plastic model), considers a constant stiffness element to represent the building above the pile (a constant load was used to compute the results presented herein, and a stiffness-controlled boundary condition is readily implemented), and seeks convergence by iterating the position of the null point to solve the load transfer distribution along the pile (the algorithm in this study monotonically changes the base displacement required to equilibrate the pile, exhibits no convergence difficulties, and naturally produces the null point as a result).

Numerical Results

The behavior of a pile subjected to cyclic thermal changes is analyzed next. The cyclic temperature change amplitude ΔT is assumed constant along the pile in agreement with results from instrumented piles (Bourne-Webb et al. 2009; Laloui et al. 2006). The pile does not have residual stresses, and a length, L, of 20 m is selected to model common thermoactive piles that reach depths where the soil temperature remains relatively unaffected by daily and seasonal weather changes (Brandl 2006).

The ultimate shaft resistance is mobilized at comparatively small relative displacements ranging from $\delta_s^* = 0.005 \cdot D$ to $0.02 \cdot D$ (Hirayama 1990; Reese 1978). In contrast, bored cast-in-place piles require a large tip displacement δ_t^* to mobilize the ultimate tip resistance. It is assumed that $\delta_s^* = 0.005 \cdot D$ and $\delta_t^* = 0.05 \cdot D$ so the critical shaft-to-base displacement ratio is $\delta_t^*/\delta_s^* = 10$. Table 2 summarizes the set of parameters used in the numerical simulation.

The vertical effective stress at the ith-element middle point z_i (m) is herein assumed to be equal to $\sigma'_{vi} = \gamma \cdot z_i$, where γ (N/m^3) is the soil unit weight. For bored piles, the coefficient of horizontal stress can be estimated as $K_0 = (1 - \sin\varphi)$, and the pile-soil interfacial friction coefficient along the rough concrete-soil interface is assumed to be $\mu = \tan\varphi$, where φ is the soil friction angle. Thus, the ultimate pile shaft resistance S^{ult} (N) is

$$S^{\text{ult}} = L_0 \cdot \pi \cdot D \cdot \sum_i^N s_i^{\text{ult}} = \frac{L^2}{2} \cdot \pi \cdot D \cdot K_0 \cdot \mu \cdot \gamma \quad (9)$$

Load-Transfer Curves

Fig. 1(b) compares the load-transfer curves after static loading and cyclic thermal loading for a temperature change amplitude

Table 1. Governing Dimensionless Ratios

Dimensionless ratios	Mathematical expression
Relative pile-to-interface stiffness	$[Q^{\text{ult}} - L/(D^2 - E)]/\delta_s^*$
Normalized free thermal elongation	$\Delta^T/\delta_s^* = (\alpha - \Delta T - L)/\delta_s^*$
Relative shaft-to-base critical displacement	δ_s^*/δ_b^*
Static factor of safety	$\text{FS} = Q^{\text{ult}}/Q^{\text{head}}$
Relative shaft-to-tip ultimate resistance	$S^{\text{ult}}/Q_t^{\text{ult}}$
Normalized tip resistance	$Q_t^{\text{ult}}/(\gamma - L - D^2)$
Pile slenderness	L/D
Normalized critical shaft displacement	δ_s^*/D
Coefficient of earth pressure at rest	K_0
Interface friction coefficient	μ

Table 2. Parameters Used in Numerical Simulations

Parameter	Symbol	Units	Value
Pile diameter[a]	D	m	1.0
Pile Young's modulus[b]	E	GPa	30
Pile thermal expansion coefficient	α	$10^{-5}/^\circ\text{C}$	1
Critical shaft displacement	δ_s^*	m	$0.005\,D$
Critical base displacement	δ_b^*	m	$0.05\,D$
Pile length	L	m	20
Soil unit weight	γ	kN/m^3	18

[a]Not smaller than 0.6 m to allow space for the heat exchanger tubing (data from McCartney 2011).
[b]Equivalent to RC (data from Laloui et al. 2006).

J. Geotech. Geoenviron. Eng. 2014.140.

$\Delta T = 20°C$, shaft-to-ultimate resistance ratio $S^{ult}/Q^{ult} = 0.5$, and static-to-ultimate load ratio $Q^{head}/Q^{ult} = 0.5$, i.e., FS = 2.0. The distribution of the pile axial force Q, mobilized side friction s, and relative displacement δ evolve with the number of thermal cycles. Heating expands the upper part of the pile upwards and the lower part downward. Thermal contraction upon cooling partially reverses this trend, and plastic displacements accumulate. There is a point of zero displacement in every thermal cycle; this point moves upwards with the number of thermal cycles.

Shaft-Bearing versus End-Bearing Piles

Fig. 2(a) compares the evolution of pile head displacement with the number of thermal cycles in both end-bearing ($S^{ult}/Q^{ult} = 0.2$) and shaft-bearing piles ($S^{ult}/Q^{ult} = 0.7$). Pile head displacements are normalized by the critical relative displacement required to mobilize the pile-soil interface shear strength $\delta_s^* = 5$ mm. This value is similar to the free thermal elongation of the unconstrained pile $\Delta^T = \alpha \cdot \Delta T \cdot L = 4$ mm when the temperature change amplitude is $\Delta T = 20°C$. End-bearing and shaft-bearing piles with low static load Q^{head} (the normalized head load is $Q^{head}/Q^{ult} = 0.2$; FS = 5) do not accumulate permanent displacements after the static load is applied. However, piles with a low factor of safety ($Q^{head}/Q^{ult} = 0.8$; FS = 1.25) accumulate displacements as the number of thermal cycles increases, tending to an asymptotic permanent displacement at the head of the pile δ_1. The end-bearing pile settles less than the shaft-bearing pile and reaches the asymptotic displacement at fewer cycles for similar normalized head loads.

Fig. 2(b) compares asymptotic pile head displacements δ_1 as a function of the normalized head load $Q^{head}/Q^{ult} = FS^{-1}$ with static load-displacement curves. Results show that thermal cycles induce asymptotic pile settlements if the static load exceeds $Q^{head}/Q^{ult} \sim 0.3$ for end-bearing piles or $Q^{head}/Q^{ult} \sim 0.7$ for shaft-bearing piles. The asymptotic load-displacement curves are parallel to the static curves, and the shifts are linearly proportional to the temperature change amplitude ΔT.

Pile Displacement with Thermal Cycles

Piles with a high head load Q^{head}/Q^{ult} and a low factor of safety accumulate gradually decreasing deformations until reaching an asymptotic settlement δ_1 or *shakedown* state. The trend of pile head displacement δ_1 versus the number of thermal cycles N_c can be fitted with an exponential function in terms of the head displacement for the static load $\delta_1|_{Nc=1}$ and the asymptotic head displacement $\delta_1|_{Nc\to\infty}$

$$\delta_1 = \delta_1|_{Nc\to\infty} + \left(\delta_1|_{Nc=1} - \delta_1|_{Nc\to\infty}\right)\exp(-\beta \cdot N_c) \qquad (10)$$

The exponent β captures the convergence rate toward the asymptotic pile head displacement and decreases as the shaft-to-ultimate resistance ratio S^{ult}/Q^{ult} increases (Fig. 3). The critical number of cycles N_c^* required to achieve 63% of the pile settlement from the initial static displacement to the asymptotic displacement ($\delta_1|_{Nc\to\infty} - \delta_1|_{Nc=1}$) can be obtained from Eq. (10) because $N_c^* = 1/\beta$. For example, an end-bearing pile ($S^{ult}/Q^{ult} = 0.2$) with a normalized head load $Q^{head}/Q^{ult} = 0.8$ (FS = 1.25) has an exponent, β, of 1.1 and will experience most of the thermally induced settlement within the first thermal cycle ($N_c^* \sim 1$); in contrast, a shaft-bearing pile ($S^{ult}/Q^{ult} = 0.7$) with static load $Q^{head}/Q^{ult} = 0.8$

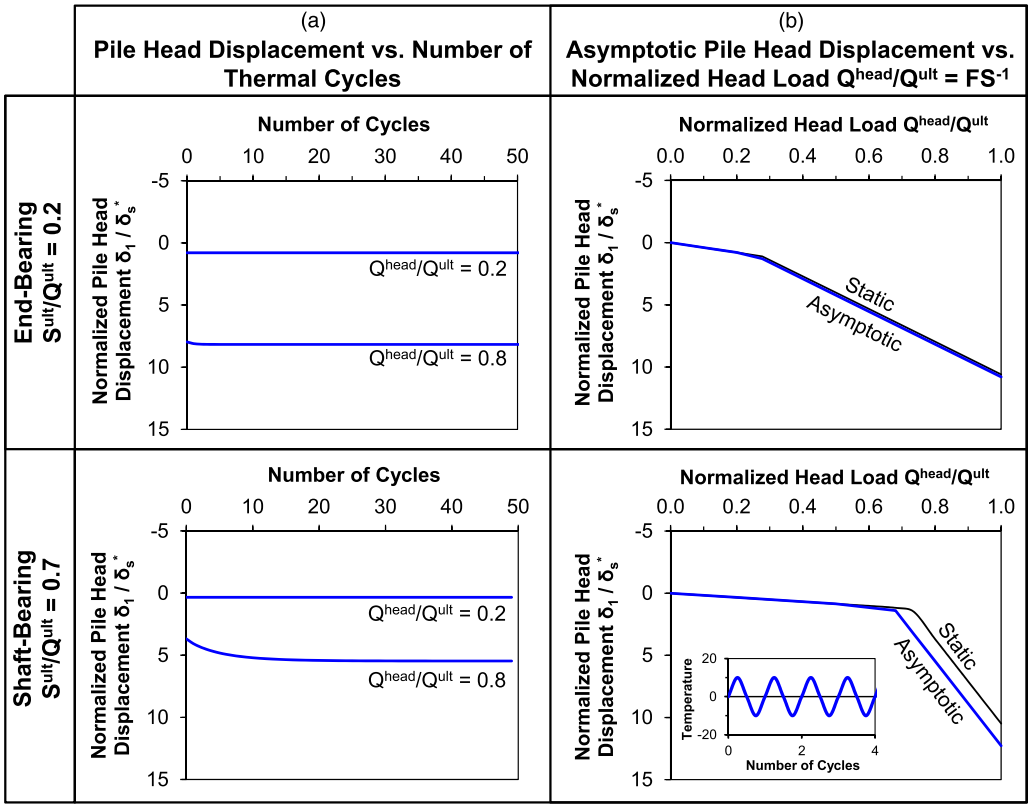

Fig. 2. Evolution of pile head displacements and asymptotic values for end- and shaft-bearing piles subjected to thermal cycles; temperature change amplitude is $\Delta T = 20°C$, and ultimate pile capacity is $Q^{ult} = 3{,}750$ kN; note that pile parameters are found in Table 2; ultimate tip resistance is $Q_t^{ult} = Q^{ult} - S^{ult}$

J. Geotech. Geoenviron. Eng. 2014.140.

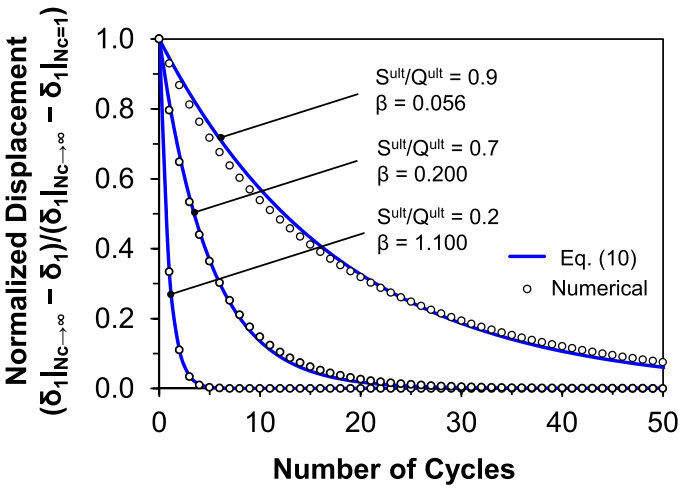

Fig. 3. Evolution of the normalized pile head displacement with the number of thermal cycles for various shaft-to-ultimate resistance ratios S^{ult}/Q^{ult}; Eq. (10) defines exponent β

has an exponent, β, of 0.2 and will require $N_c^* \sim 5$ thermal cycles to experience 63% of the thermally induced settlement.

Other Observations

Additional parametric studies were conducted to explore a wider range of conditions. Observations from these studies include

- Purely shaft-bearing piles ($S^{ult}/Q^{ult} = 1$) subjected to thermal cycles and purely end-bearing piles ($S^{ult}/Q^{ult} = 0$) deform elastically with thermal cycles and expand upwards if the static load Q^{head} remains constant.
- Thermal effects are exacerbated if the critical displacement δ^* required to mobilize the pile-soil interface shear strength is small, i.e., Δ^T/δ_s^* is large.
- Larger-diameter piles (smaller L/D) are less susceptible to thermal effects due to the larger critical displacement δ^* required to mobilize shaft and base ultimate capacities.

As noted in the introduction, this numerical algorithm does not account for soil thermal consolidation and changes in horizontal effective stress that may develop around the pile.

Conclusions

Numerical results for the long-term response of thermoactive piles subjected to thermal cycles show that thermally induced pile displacements can result in the accumulation of plastic displacements with the number of thermal cycles. Although the ultimate pile capacity may remain constant, the accumulation of thermally induced plastic displacements can affect the long-term thermoactive pile performance. Cumulative plastic displacements approach shakedown conditions with asymptotic displacements that are proportional to the temperature change amplitude when the mean value of the thermal cycles is zero.

Shaft-bearing piles develop larger settlements at a higher number of cycles, whereas end-bearing piles reach smaller asymptotic displacements at fewer thermal cycles. In the limit, an end-bearing pile without shaft resistance does not accumulate thermally induced plastic displacements.

In cases prone to shakedown, the evolution of the pile head displacement follows an exponential function in terms of the number of thermal cycles. Preliminary results suggest that most of the thermally induced plastic displacements take place in the first few cycles, typically less than 10–20 cycles for standard applications.

Acknowledgments

Support for this research was provided by the Fulbright U.S.-Chile Equal Opportunities Scholarship Program, the U.S. Department of Energy, and the Goizueta Foundation. Francisco Santamarina edited the manuscript.

References

Amatya, B. L., Soga, K., Bourne-Webb, P. J., Amis, T., and Laloui, L. (2012). "Thermo-mechanical behaviour of energy piles." *Geotechnique*, 62(6), 503–519.

Bourne-Webb, P. J., Amatya, B., and Soga, K. (2012). "A framework for understanding energy pile behaviour." *Proc. ICE–Geotechnical Engineering*, 166(2), 170–177.

Bourne-Webb, P. J., Amatya, B., Soga, K., Amis, T., Davidson, C., and Payne, P. (2009). "Energy pile test at Lambeth College, London: Geotechnical and thermodynamic aspects of pile response to heat cycles." *Geotechnique*, 59(3), 237–248.

Brandl, H. (2006). "Energy foundations and other thermo-active ground structures." *Geotechnique*, 56(2), 81–122.

Coyle, H. M., and Reese, L. C. (1966). "Load transfer for axially loaded piles in clay." *J. Soil Mech. and Found. Div.*, 92(2), 1–26.

Hirayama, H. (1990). "Load-settlement analysis for bored piles using hyperbolic transfer functions." *Soils Found.*, 30(1), 55–64.

Knellwolf, C., Peron, H., and Laloui, L. (2011). "Geotechnical analysis of heat exchanger piles." *J. Geotech. Geoenviron. Eng.*, 10.1061/(ASCE)GT.1943-5606.0000513, 890–902.

Laloui, L., Nuth, M., and Vulliet, L. (2006). "Experimental and numerical investigations of the behaviour of a heat exchanger pile." *Int. J. Numer. Anal. Methods Geomech.*, 30(8), 763–781.

McCartney, J. (2011). "Engineering performance of energy foundations." *Pan-Am CGS Geotechnical Conf.*, International Society for Soil Mechanics and Geotechnical Engineering, and the Canadian Geotechnical Society, Toronto.

Poulos, H. G., and Davis, E. H. (1980). *Pile foundation analysis and design*, Wiley & Sons, New York.

Reese, L. C. (1978). "Design and construction of drilled shafts." *J. Geotech. Engrg. Div.*, 104(1), 91–116.